Spatiotemporal Hub Identification in Brain Network by Learning Dynamic Graph Embedding on Grassmannian Manifold

Defu Yang[1,2], Hui Shen[3], Minghan Chen[4], Yitian Xue[3], Shuai Wang[1], Guorong Wu[2], and Wentao Zhu[3](✉)

[1] School of Automation, Hangzhou Dianzi University, Hangzhou, China
[2] Department of Psychiatry, University of North Carolina at Chapel Hill, Chapel Hill, USA
[3] Research Center for Augmented Intelligence, Zhejiang Lab, Hangzhou, China
wentao.zhu@zhejianglab.com
[4] Department of Computer Science, Wake Forest University, Winston-Salem, NC, USA

Abstract. Advancements in neuroimaging technology have made it possible to measure the connectivity evolution between different brain regions over time. Emerging evidence shows that some critical brain regions, known as hub nodes, play a significant role in updating brain network connectivity over time. However, current spatiotemporal hub identification is built on static network-based approaches, where hub regions are identified independently for each temporal brain network without considering their temporal consistency, and fails to align the evolution of hubs with changes in connectivity dynamics. To address this problem, we propose a novel spatiotemporal hub identification method that utilizes dynamic graph embedding to distinguish temporal hubs from peripheral nodes. Specially, to preserve the time consistency information, we put the dynamic graph embedding learning upon a smooth physics model of network-to-network evolution, which mathematically expresses as a total variation of dynamic graph embedding with respect to time. A novel Grassmannian manifold optimization scheme is further introduced to learn the embeddings accurately and capture the time-varying topology of brain network. Experimental results on real data demonstrate the highest temporal consistency in hub identification, surpassing conventional approaches.

1 Introduction

The human brain is a complex and economically organized system, consisting of interconnected regions that form a hierarchical brain network [1]. Understanding the topology of these networks is crucial for gaining insight into brain function and behavior [2]. Like many other real networks, brain network exhibits characteristics of a small-world and free-scale organization, where there are a small number of hub nodes that are densely connected to other peripheral regions [3, 4]. Recent studies show that hub nodes play a central role in adapting brain network connectivity to meet task demands [2, 5]. It has

D. Yang and H. Shen—These authors contributed equally.

H. Greenspan et al. (Eds.): MICCAI 2023, LNCS 14221, pp. 394–402, 2023.
https://doi.org/10.1007/978-3-031-43895-0_37

been also observed that most neurodegenerative and neuropsychiatric diseases are associated with alterations in dynamic functional connectivity (dFC) that occur selectively on hub nodes [6–9]. Therefore, accurate identification of hub nodes from brain networks, particularly in a dynamic scenario, is essential for understanding brain development and the neurodegenerative process.

In network science, hub nodes are often classified as provincial or connector hubs based on the information of network modules [4]. Provincial hubs have high connectivity within a single module, while connector hubs link multiple communities and play a more critical role in the overall network organization [4, 10]. With the consensus that damage to connector hubs can result in a wider disruption of the brain than damage to provincial hubs [11–13], identifying connector hubs is location-wise and function-wise more important. Multiple hub identification methods have been proposed and can be grouped into univariate-sorting-based [4, 14, 15] and multivariate-learning-based approaches [16]. The former involves selecting the top nodes ranked by certain nodal centrality, while the latter jointly identifies a set of critical nodes by learning topological features represented by low-dimensional graph embeddings.

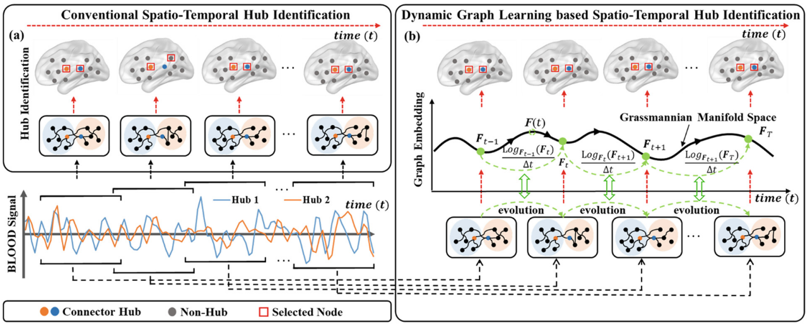

Fig. 1. Conventional (a) vs. dynamic graph embedding (b) approaches for spatiotemporal hub identification. In the proposed framework, temporal networks evolve from the previous state instead of being treated as independent static networks. Through learning a dynamic graph embedding that follows a physics-based network evolution model, the identified temporal hubs consistently align with dynamically changing connectivity.

Although various methods exist for identifying hub nodes in brain networks, there is a notable gap in effective approaches for dynamic scenarios. One common strategy is to treat each network as a separate static network and then use existing hub identification methods for each sliding window independently to obtain a set of spatiotemporal hub nodes, as illustrated in Fig. 1(a). Where a dynamic sequence of time-varying networks is generated applying a sliding window technique to BOLD signals in fMRI imaging data. While efficient, this approach lacks an in-depth exploration of how the topological evolution is linked to hub regions, and it often produces low-consistency hubs due to a low signal-to-noise ratio, as depicted in Fig. 1(a).

To address these challenges, we propose a novel learning-based spatiotemporal hub identification method. Unlike existing approaches that treat each temporal network as an independent static network, our method jointly identifies a set of temporal hub nodes using a dynamic graph embedding. Specially, due to dynamic graph embedding vectors [17–19] are the underlying representation of time-varying brain network, we can easily cast the network-to-network evolution over time as a total variation of dynamic graph embedding with respect to time, where each temporal graph embedding are not independent. Furthermore, in Fig. 1(b), as each temporal graph embedding vector is an instance residing on a Grassmannian manifold [19], we leverage the Grassmannian manifold optimization scheme to learn the dynamic graph embeddings. Overall, our spatiotemporal hub identification method ensures the temporal consistency of hub nodes over time while aligning the temporal hubs with the dynamic connectivity evolution in real time. We evaluate our proposed method on both synthetic and real brain network data, and results show that it outperforms conventional approaches.

2 Method

2.1 Dynamic Graph Embedding Learning

Dynamic Brain Network. Suppose we observe a time-varying brain network consisting of N brain regions, we define the network over time as a dynamic graph $\mathcal{G} = (\mathcal{V}, \mathcal{E}, \mathcal{T})$, where $\mathcal{V} = \{\boldsymbol{V}(t)\}_{t\in\mathcal{T}}$ is the node set over time, $\mathcal{E} = \{\boldsymbol{E}(t)\}_{t\in\mathcal{T}}$ is a collection of edges over time, and $\mathcal{T}$ is the time span. For each temporal point $t \in \mathcal{T} = [0, T]$, there is a graph snapshot $\mathbb{G}_t$ of N nodes with the node-to-node connectivity degrees encoded in an $N \times N$ adjacency matrix, denoted as $\boldsymbol{W}(t) = \left[w_{ij}\right]_{i,j=1}^{N}$.

Temporal Hub Identification. Given a temporal network $\mathbb{G}_t$, our goal is to find K hubs in each temporal network. The locations of these temporal hubs are indexed by a binary diagonal matrix $\boldsymbol{S}(t) = diag(\boldsymbol{s}(t)) = diag([s_i]_{i=1}^{N})$, where $s_i = 0$ indicates the i^{th} node is a hub, and $s_i = 1$ otherwise. To achieve this, we require the latent temporal graph embedding $\boldsymbol{F}(t) \in \mathbb{R}^{N\times P}(P < N, \boldsymbol{F}(t)^{\boldsymbol{T}}\boldsymbol{F}(t) = \boldsymbol{I}_{P\times P},)$ for each temporal network $\boldsymbol{W}(t)$ should yield a distinct separation between connector hub nodes and the peripheral nodes. To link the learning of $\boldsymbol{F}(t)$ with the optimization of hub selection indicator $\boldsymbol{s}(t)$, we adopt the following objective function:

$$\arg\min_{\boldsymbol{F}(t),\boldsymbol{S}(t)} tr\Big(\boldsymbol{F}^T(t)\boldsymbol{L_s}(t)\boldsymbol{F}(t)\Big) = tr\Big(\boldsymbol{F}^T(t)(\boldsymbol{D_s}(t) - \boldsymbol{S^T}(t)\boldsymbol{W}(t)\boldsymbol{S}(t))\boldsymbol{F}(t)\Big), \quad (1)$$

where $\boldsymbol{L_s}(t) = \boldsymbol{D_s}(t) - \boldsymbol{S^T}(t)\boldsymbol{W}(t)\boldsymbol{S}(t)$ is the temporal degraded Laplacian matrix and $\boldsymbol{D_s}(t) = diag\left(\left[\sum_{j=1}^{N} s_i w_{ij} s_j\right]_{i=1}^{N}\right)$ is the diagonal matrix. The trace norm, $tr\Big(\boldsymbol{F}^T(t)\boldsymbol{L_s}(t)\boldsymbol{F}(t)\Big) = \sum_{i,j}^{N} s_i w_{ij} s_j \|\boldsymbol{F_i}(t) - \boldsymbol{F_j}(t)\|_2^2$, measures the smoothness of graph embedding in the context of the network topology governed by $\boldsymbol{L_s}(t)$, where $\boldsymbol{F_i}(t)$ and $\boldsymbol{F_j}(t)$ are the temporal embedding on nodes v_i and v_j. Suppose v_i is the temporal hub node and v_j is the linked non-hub node. Specifically, we want the distance term $\|\boldsymbol{F_i}(t) - \boldsymbol{F_j}(t)\|_2^2$ to be as large as possible to separate hub and peripheral nodes, while expecting that connector hubs, which have a higher connectivity degree than peripheral nodes, will have a large weight w_{ij}. Thus, identifying hub is searching for a solution that excluding all K hub nodes (let $s_i = 0$) from the objective function to minimize the trace norm.

Physics-Based Network Evolution Model. Since a temporal network evolves from the previous temporal state, the physics network-to-network evolution model can be mathematically described as follows:

$$\boldsymbol{F}(t) = \boldsymbol{F}(t - \Delta\tau) + \frac{\partial \boldsymbol{F}(t)}{\partial t}\Delta\tau, \tag{2}$$

where $\Delta\tau$ is the time interval and $\frac{\partial \boldsymbol{F}(t)}{\partial t}$ denotes the network-to-network evolution rate. In the context of neurobiological signals, the evolution of network connectivity is a smooth process rather than a mutational change. This means that as the time interval between two consecutive network states approaches zero, the 2-norm difference between two consecutive networks ($\boldsymbol{F}(t)$ and $\boldsymbol{F}(t-\Delta\tau)$) approaches a finite value, i.e., $\lim_{\Delta\tau\to 0} \| \frac{\boldsymbol{F}(t)-\boldsymbol{F}(t-\Delta\tau)}{\Delta\tau} \|_2^2 \neq \infty$. Therefore, to ensure that the network connectivity evolves smoothly over time, the evolution of $\boldsymbol{F}(t)$ is subject to the minimization constraint of the integral of $\boldsymbol{F}(t)$ change rate over the entire time period, i.e., $\int_0^T \| \frac{\partial \boldsymbol{F}(t)}{\partial t} \|_2^2 dt$.

Spatiotemporal Hub Identification. By integrating the physics network-to-network evolution model, the spatiotemporal hub identification for the entire time series can be mathematically represented as:

$$\arg\min_{\boldsymbol{F}(t),\boldsymbol{S}(t)} \int_0^T tr\Big(\boldsymbol{F}^T(t)\Big(\boldsymbol{D}_s(t) - \boldsymbol{S}^T(t)\boldsymbol{W}(t)\boldsymbol{S}(t)\Big)\boldsymbol{F}(t)\Big)dt + \alpha\int_0^T \|\frac{\partial \boldsymbol{F}(t)}{\partial t}\|_2^2 dt, \tag{3}$$

which includes two terms: the identification of temporal hub sets $\boldsymbol{S}(t)$ over time using the learned dynamic graph embedding $\boldsymbol{F}(t)$, and the regularization term that enforces the smoothness of $\boldsymbol{F}(t)$ evolution over time. The scalar parameter α controls the trade-off between the two terms.

2.2 Optimization on Grassmannian Manifold

Equation (3) involves an integral-differential form with respect to (*w.r.t*) $\boldsymbol{F}(t)$ and is hard to solve directly. To address this issue, we divide the entire time series into M segments with an interval of $\Delta t = \frac{T}{M}$, where $\lim_{M\to\infty} \frac{T}{M} = 0$. This allows us to decompose Eq. (3) into a linear discrete model based on the integration definition:

$$\arg\min_{\boldsymbol{F}(t_m),\boldsymbol{S}(t_m)} \sum_{m=1}^{M}\left(tr\Big(\boldsymbol{F}^T(t_m)\boldsymbol{L}_s(t_m)\boldsymbol{F}(t_m)\Big) + \alpha\|\frac{\Delta\boldsymbol{F}(t_m)}{\Delta t}\|_2^2\right)\Delta t. \tag{4}$$

Since Eq. (4) is not a convex function, we adopt an alternative approach to jointly optimize $\boldsymbol{S}(t_m)$ and $\boldsymbol{F}(t_m)$ in the following.

Optimizing Dynamic Graph Embedding on Grassmannian Manifold. According to [19], each temporal graph embedding $\boldsymbol{F}(t_m)$ can be represented as an instance on the Grassmannian manifold $\mathcal{I}(P, N) \in \mathbb{R}^{N\times P}$, which makes the classic Euclidean space unsuitable for measuring the variation of $\Delta\boldsymbol{F}(t_m)$. In the context of physics, $\|\Delta\boldsymbol{F}(t_m)\|_2^2$ signifies the evolving variation from the temporal state t_{m-1} to t_m, see Fig. 1(b). In the Grassmannian manifold space, $\|\Delta \boldsymbol{F}(t_m)\|_2^2$ can be accurately measured by the squared geodesic distance $Log_{\boldsymbol{F}(t_m)}(\boldsymbol{F}(t_{m-1})) = P - tr(\boldsymbol{F}(t_m)\boldsymbol{F}(t_m)^T\boldsymbol{F}(t_{m-1})\boldsymbol{F}(t_{m-1})^T)$. Therefore, the optimization of Eq. (4) $w.r.t$ $\boldsymbol{F}(t_m)$ is as follows:

$$\boldsymbol{J} = \arg\min_{\boldsymbol{F}(t_m)} \sum_{m=1}^{M} tr\Big(\boldsymbol{F}^T(t_m)\boldsymbol{L_s}(t_m)\boldsymbol{F}(t_m) - \beta\boldsymbol{F}(t_m)\boldsymbol{F}(t_m)^{\boldsymbol{T}}\boldsymbol{F}(t_{m-1})\boldsymbol{F}(t_{m-1})^{\boldsymbol{T}}\Big), \quad (5)$$

where $\beta = \frac{\alpha}{\Delta t^2}$ is a scaler parameter. Following the optimization framework in [19], we calculate the Grassmannian gradient $\Delta_{\boldsymbol{F}(t_m)}$ of each temporal $\boldsymbol{F}(t_m)$ by projecting the Euclidean gradient $\frac{\partial \boldsymbol{J}(\boldsymbol{F}(t_m))}{\partial \boldsymbol{F}(t_m)} = 2(\boldsymbol{L_s}(t_m) - \sum_{i=-1,i\neq 0}^{1}\beta\boldsymbol{F}(t_{m+i})\boldsymbol{F}(t_{m+i})^{\boldsymbol{T}})\boldsymbol{F}(t_m)$ onto the tangent space via the orthogonal projection [19]:

$$\Delta_{\boldsymbol{F}(t_m)} = (\boldsymbol{I}_{N\times N} - \boldsymbol{F}(t_m)\boldsymbol{F}(t_m)^{\boldsymbol{T}})\frac{\partial J(\boldsymbol{F}(t_m))}{\partial \boldsymbol{F}(t_m)} \quad (6)$$

Given $\Delta_{\boldsymbol{F}(t_m)}$, we update the modified $\boldsymbol{F}(t_m)$ using an exponential mapping operation [19]:

$$\boldsymbol{F}(t_m) = exp\big(-\Delta_{\boldsymbol{F}(t_m)}\big) = [\boldsymbol{F}(t_m)\boldsymbol{V}diag(\cos(\varepsilon\boldsymbol{\Sigma})) + \boldsymbol{U}diag(\sin(\varepsilon\boldsymbol{\Sigma}))]\boldsymbol{V}^{\boldsymbol{T}}, \quad (7)$$

where $\boldsymbol{U}$, $\boldsymbol{\Sigma}$, and $\boldsymbol{V}$ are derived from the compact singular value decomposition (SVD) of $-\Delta_{\boldsymbol{F}m}$, i.e., $-\Delta_{\boldsymbol{F}m} = \boldsymbol{U\Sigma V^T}$. ε is a scalar parameter controlling the step size of optimization.

Optimizing Temporal Hub Node Set. After updating$\boldsymbol{F}(t_m)$, the energy function of Eq. (4) can be rearranged as Eq. (8) with $\boldsymbol{S}(t_m) = diag(\boldsymbol{s}(t_m))$:

$$\underset{\boldsymbol{s}(t_m)}{argmin} tr(\boldsymbol{s}(t_m)^T\boldsymbol{H}(t_m)\boldsymbol{s}(t_m)), \quad (8)$$

where $\boldsymbol{H}(t_m) = \left[h_{ij}\right]_{i,j}^{N}$ is an $N\times N$ matrix, and each element $h_{ij} = w_{ij}\|\boldsymbol{F_i}(t_m) - \boldsymbol{F_j}(t_m)\|_2^2$ represents the distance between the temporal graph embedding $\boldsymbol{F}(t_m)$ at the i^{th} and j^{th} nodes. The optimal set of temporal hub nodes $\boldsymbol{s}$ at the t_m temporal point can be achieved using the convex optimization scheme proposed in [16].

3 Experiments and Results

We assess the performance of our spatiotemporal hub identification method on both simulated and real network data. Our proposed method, named Dynamic-Graph-Embedding-based method, not only learns the topological features of each temporal network but also jointly learns the evolving consistency pattern on the entire dynamic sequence. We compare our method with conventional approaches: the classic sorting-based hub identification method that uses nodal betweenness centrality [20] (referred to as Sorting-Betweenness-based method), and the multivariate-learning-based hub identification that learns the topological property independently for each temporal network (Graph-Embedding-based method [16]).

3.1 Accuracy and Robustness on Synthesized Network Data

Data Preparation. A set of synthesized time-variant networks were generated by the folling steps: (1) initialize a network with a specified number of nodes and connections; (2) set an evolution ratio (updated/total) to simulate the gradual process of network evolution. This involves keeping a fixed proportion of connections in the final state, while updating the remaining connections to generate the evolved network. Figure 2 shows toy examples of the synthesized time-varying network.

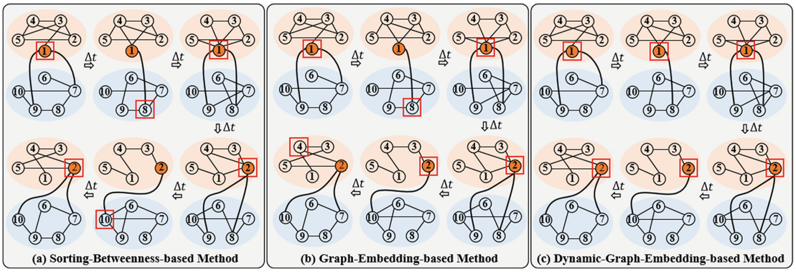

Fig. 2. Comparison of spatiotemporal hub identification using Sorting-Betweenness-based (a), Graph-Embedding-based (b), and Dynamic-Graph-Embedding-based (c) methods. The orange node represents the synthesized hub, while the other nodes are non-hubs.

Accuracy. A sequence of dynamic networks containing 6 temporal states was considered, with each temporal network containing two modules. Figure 2(a)-(c) illustrates the hubs identified for each temporal network using Sorting-Betweenness-based, Graph-Embedding-based, and Dynamic-Graph-Embedding-based methods, which are highlighted in a red box. The synthesized hubs (orange node) in the first three temporal states and the last three temporal states were labeled as node #1 and #2, respectively. It is evident that our proposed spatiotemporal hub identification approach can accurately identify the hub by incorporating the physics-based network evolution pattern.

Robustness. To further quantify the robustness of our proposed spatiotemporal hub identification method, we varied the complexity of network evolution and the network topology by changing the evolution ratio and hub number. Each time-varying network underwent 50 evolutions. The performance was evaluated by changing the evolution ratio from 40% to 70% and increasing the hub number in each temporal network while fixing other variables. We repeated the process 50 times and reported the overlap ratio between the identified temporal hubs and the ground truth across the entire dynamic sequence. Figure 3 shows that our proposed method consistently outperformed conventional methods, demonstrating its superior reliability.

3.2 Evaluation of Hub Identification on Real Brain Networks

Data Preparation. A total of 125 subjects consisting of 63 normal control (NC) and 62 obsessive-compulsive disease (OCD) were selected from an obsessive-compulsive

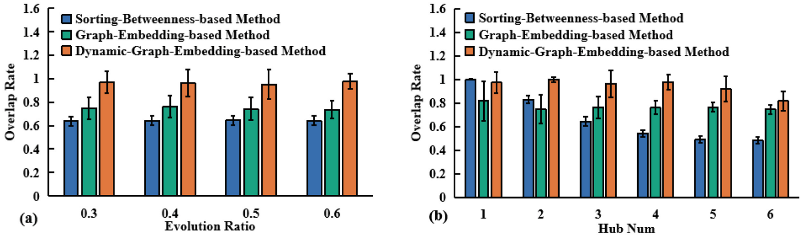

Fig. 3. Overlap ratio between ground truth and identified temporal hubs w.r.t evolution ratio (a) and hub number (b), using Sorting-Betweenness-based (blue), Graph-Embedding-based (green), and our proposed Dynamic-Graph-Embedding-based (orange) methods. (Color figure online)

disease (OCD) study to evaluate the consistency performance and diagnosis value. We used the AAL atlas to partition the brain into 90 regions of interest (ROIs). By dividing the entire time course of BOLD signals into three temporal time segments with a window size of 50 s, each subject obtained a dynamic sequence consisting of three frames of 90×90 adjacent matrix.

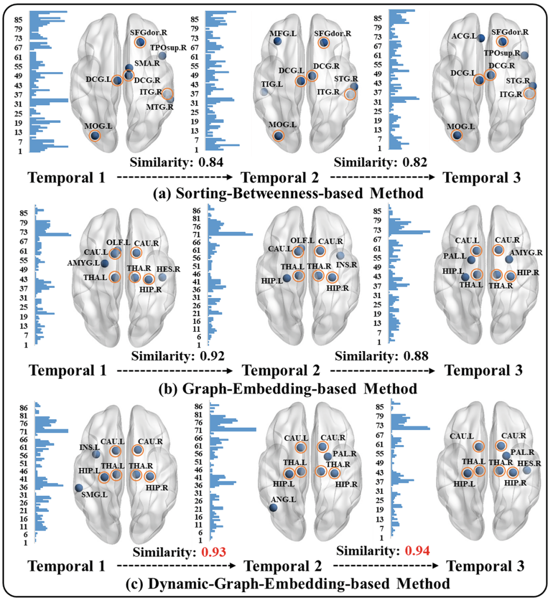

Fig. 4. Comparison of hub topology persistency across temporal states using Sorting-Betweenness-based (a), Graph-Embedding-based (b), and Dynamic-Graph-Embedding-based (c) methods. The orange circle represents the common hubs across temporal states. The left panel shows a count histogram of network nodes selected as hubs at each temporal state across subjects, while the right panel displays the most representative hub nodes voted across subjects.

Consistency of Hub Topology. We employed conventional engineering methods and our proposed spatiotemporal hub identification technique on each sliding window across subjects, as depicted in Fig. 4. The emerging evidence suggests that hubs remain stable even when switching brain states between tasks [5, 11]. Thus, it is also reasonable for us to hypothesize that hubs remain stable underlying a resting-state environment. Our proposed Dynamic-Graph-Embedding-based method yielded the highest consistency of hub locations across temporal states (6 common hubs), followed by the Graph-Embedding-based (5 common hubs) and Sorting-Betweenness-based methods (4 common hubs). To further quantify the similarity, we calculated the covariance of the count histogram between the last and current temporal states, and our method exhibited the highest similarity (Fig. 4(c)).

(a) Sorting-Betweenness-based Method

Hub	Feature1	Feature2	Feature1	Feature2	Hub
SFGdor.R	-	-	**	***	STG.R
DCG.L	-	*	*	*	TPOsup.R
DCG.R	-	-	-	-	MTG.R
MOG.L	-	-	-	-	ITG.R

(b) Graph-Embedding-based Method

Hub	Feature1	Feature2	Feature1	Feature2	Hub
HIP.L	-	-	**	**	THA.L
HIP.R	***	**	**	*	THA.R
CAU.L	*	-	**	**	OLF.L
CAU.R	*	**	*	-	AMYG.L

(c) Dynamic-Graph-Embedding-based Method

Hub	Feature1	Feature2	Feature1	Feature2	Hub
HIP.L	-	-	**	**	THA.L
HIP.R	***	**	**	*	THA.R
CAU.L	*	-	**	**	HES.R
CAU.R	*	**	*	*	PAL.R

Feature1: Local Efficiency	Feature2: Clustering Coefficient
*** $p < 0.001$	** $0.001 \le p < 0.01$
* $0.01 \le p \le 0.05$	- $p > 0.05$

Fig. 5. Statistical power at the hub nodes identified by Sorting-Betweenness-based (a), Graph-Embedding-based (b), and Dynamic-Graph-Embedding-based (c) methods. The significance after a two-sample t-test was indicated by red stars. (Color figure online)

Statistical Power of the Identified Hubs. As mounting evidence suggests that certain neurodegeneration and neuropsychiatric diseases selectively damage hub regions, we performed a two-sample t-test to assess the statistical power of the identified hub. We identified hubs for each subject at each temporal point and then voted out the eight most frequently selected nodes as the common hubs across the entire temporal series, as shown in Fig. 5. The significance was indicated by red stars. Our proposed spatiotemporal hub identification method yielded more hub nodes manifesting significant differences specific to OCD compared to the other two methods (Fig. 5(a)).

4 Conclusion

This paper introduces a novel spatiotemporal hub identification method. Our approach integrates the evolution model of network connectivity to ensure the consistency of dynamic graph embedding over time. The results on both simulated and real data are promising and suggest the great potential for investigating the role of hubs in the evolution of both task-based and resting-state-based networks.

References

1. Bullmore, E., Sporns, O.: The economy of brain network organization. Nat. Rev. Neurosci. **13**, 336 (2012)
2. Bertolero, M.A., Yeo, B.T.T., Bassett, D.S., D'Esposito, M.: A mechanistic model of connector hubs, modularity and cognition. Nat. Hum. Behav. **2**, 765–777 (2018)
3. Park, H.-J., Friston, K.: Structural and functional brain networks: from connections to cognition. Science **342**, 1238411 (2013)
4. van den Heuvel, M.P., Sporns, O.: Network hubs in the human brain. Trends Cogn. Sci. **17**, 683–696 (2013)
5. Cole, M.W., Reynolds, J.R., Power, J.D., Repovs, G., Anticevic, A., Braver, T.S.: Multi-task connectivity reveals flexible hubs for adaptive task control. Nat. Neurosci. **16**, 1348–1355 (2013)
6. Pedersen, M., Omidvarnia, A., Zalesky, A., Jackson, G.D.: On the relationship between instantaneous phase synchrony and correlation-based sliding windows for time-resolved fMRI connectivity analysis. Neuroimage **181**, 85–94 (2018)
7. Lee, W.J., et al.: Regional Aβ-tau interactions promote onset and acceleration of Alzheimer's disease tau spreading. Neuron **110**, 1932–1943, e1935 (2022)
8. Achard, S., et al.: Hubs of brain functional networks are radically reorganized in comatose patients. Proc. Natl. Acad. Sci. **109**, 20608–20613 (2012)
9. Frontzkowski, L., et al.: Earlier Alzheimer's disease onset is associated with tau pathology in brain hub regions and facilitated tau spreading. Nat. Commun. **13**, 4899 (2022)
10. Fornito, A., Zalesky, A., Breakspear, M.: The connectomics of brain disorders. Nat. Rev. Neurosci. **16**, 159 (2015)
11. Buckner, R.L., et al.: Cortical hubs revealed by intrinsic functional connectivity: mapping, assessment of stability, and relation to Alzheimer's disease. J. Neurosci. **29**, 1860–1873 (2009)
12. Gratton, C., Nomura, E.M., Pérez, F., Esposito, M.D.: Focal brain lesions to critical locations cause widespread disruption of the modular organization of the brain. J. Cogn. Neurosci. **24**, 1275–1285 (2012)
13. Tu, W., Ma, Z., Zhang, N.: Brain network reorganization after targeted attack at a hub region. Neuroimage **237**, 118219 (2021)
14. Jiao, Z., Xia, Z., Cai, M., Zou, L., Xiang, J., Wang, S.: Hub recognition for brain functional networks by using multiple-feature combination. Comput. Electr. Eng. **69**, 740–752 (2018)
15. Sporns, O.: Graph theory methods: applications in brain networks. Dialogues Clin. Neurosci. **20**, 111 (2018)
16. Yang, D., et al.: Joint hub identification for brain networks by multivariate graph inference. Med. Image Anal. **73**, 102162 (2021)
17. Newman, M.E.: Modularity and community structure in networks. Proc. Natl. Acad. Sci. **103**, 8577–8582 (2006)
18. Zhou, D., Huang, J., Schölkopf, B.: Learning with hypergraphs: clustering, classification, and embedding. In: Advances in Neural Information Processing Systems, vol. 19 (2006)
19. Cetingul, H.E., Vidal, R.: Intrinsic mean shift for clustering on Stiefel and Grassmann manifolds. In: 2009 IEEE Conference on Computer Vision and Pattern Recognition, pp. 1896–1902. IEEE (2009)
20. Tijms, B.M., et al.: Alzheimer's disease: connecting findings from graph theoretical studies of brain networks. Neurobiol. Aging **34**, 2023–2036 (2013)